PERGAMON

Journal of Structural Geology 21 (1999) 449–466

JOURNAL OF STRUCTURAL GEOLOGY

Application of the Prandtl–Nadai cell model to a regional scale fault intersection: the Grésigne–Quercy block (SW France)

Jacques Ingles, Christian Dauch, Jean-Claude Soula *, Pierre Viallard, Stéphane Brusset

Université Paul Sabatier, 38 rue des Trente Six Ponts, 31400 Toulouse, France

Received 25 September 1997; accepted 12 August 1998

Abstract

The Grésigne–Quercy region is a regional-scale wedge-shaped block bounded by major conjugate strike-slip faults, where the regional shortening direction bisects the acute angle of the conjugate sets. This block is composed of a Late-Carboniferous, Permian and Mesozoic cover overlying a metasedimentary basement. This region is extensively deformed, whereas the adjacent areas which are comprised of a more rigid granitoid-rich basement are undeformed or slightly deformed. The region is also characterized by the development of a fold and thrust system near the apex and strike-slip conjugate faults in the wide end. The displacement, strain and stress patterns of the Grésigne–Quercy block are inferred on the basis of structural characteristics. These structural characteristics are evaluated in terms of the geometry, kinematics, rheology, strain conditions and stress trajectories of a Prandtl–Nadai cell. This comparison shows good agreement between the natural example and the theoretical model, except that the 'plates' constituted by the 'rigid' basement outside the cell-bounding faults are immovable, whereas in the theoretical model they move apart. This difference can explain why the fold and thrust system developed in the apical zone. This fold and thrust system propagated backwards, from the apex where the material was first locked, to the wide end of the wedge-shaped block.

1. Introduction

Since the pioneering work of Anderson (1951), it is generally considered that many faults occur as conjugate sets (see review in Johnson, 1995). Many studies have been carried out on faulting mechanisms and fault geometry but few are specifically devoted to the deformation occurring in the intersection zone of conjugate faults. These studies involve either analogue scaled model studies (Oertel, 1965; Horsfield, 1980; Odonne and Massonnat, 1992), geometrical models (Ramsay and Huber, 1987, pp. 514–515) or natural case studies at scales ranging from regional (Varnes, 1962) to mesoscopic (Odonne and Massonnat, 1992) and microscopic (Lamouroux et al., 1991). Most studies are focussed on either the geometry of the intersection (Oertel, 1965; Horsfield, 1980; Ramsay and Huber, 1987; Lamouroux et al., 1991) or the displacement and strain patterns at the contact of the faults (Varnes, 1962; Odonne and Massonnat, 1992).

In the Grésigne–Quercy region in SW France, two regional strike-slip faults intersect, and the crustal block between the two faults has been shortened in a direction parallel to the acute bisector of the faults. This v-shaped crustal block consists of a Mesozoic sedimentary cover overlying a metasedimentary basement, rocks which are more ductile than the adjacent areas made up of a granitoid-rich 'rigid' basement. The region between faults is extensively deformed, whereas the adjacent areas are undeformed or slightly deformed. The deformation of the cover is also characterized by the development of a fold and thrust system near the apex of the v-shaped area and strike-slip conjugate faults in its wide end.

* Corresponding author. *E-mail address*: geostruc@cict.fr

0191-8141/99 $ - see front matter
PII: S0191-8141(99)00008-5

These rather unusual characteristics, and especially the rheological contrast between the ductile wedge-shaped block and the undeformed 'rigid' basement enable us to compare the deformation patterns within this wedge-shaped block with the predictions of a wedge-shaped Prandtl–Nadai cell (Prandtl, 1924; Hill, 1950; Nadai, 1950; Freudenthal and Geringer, 1958; Kanizay, 1962; Varnes, 1962). In the first part of this study, we describe briefly the lithology of the Grésigne and adjacent areas and present an analysis of strain trajectories and displacements inferred from large-scale and minor structures. In the second part, we propose a mechanical model based on the similarities and differences between the studied area and the predictions of a variation of the Prandtl–Nadai theoretical model.

2. Part I—geological characteristics

2.1. Geological context

The Grésigne–Quercy area, which forms part of the northern foreland of the Pyrenees, is situated on the south-western boundary of the French Massif Central to the north of the Aquitaine basin (Fig. 1). It constitutes the south-eastern part of the Quercy block which is covered by a blanket of sub-horizontal Mesozoic carbonates ('Causses du Quercy') overlying late Carboniferous and Permian deposits and the pre-Hercynian basement. The Grésigne–Quercy area is bounded to the east by the NNE–SSW-trending Villefranche fault and to the west by the NNW–SSE-trending West Quercy Fault (Durand-Delga, 1979; Dauch et al., 1989).

The Villefranche fault is part of one of the major fault zones in the French Hercynian basement. It constitutes the southern part of the Grand Sillon Houiller of the Massif Central which runs north as far as the eastern Paris basin (Sancerre fault). To the south, it continues down to the Pyrenees through the Muret fault (Fig. 1). Large left-lateral displacements occurred during Late Carboniferous time (40–70 km according to Grolier and Letourneur, 1968). The displacements during Cenozoic time were smaller.

The displacements along the West Quercy Fault were essentially right-lateral during Eocene to Oligocene time (Durand-Delga, 1979; Gaillard and Masse, 1980; Pélissié, 1982). The West Quercy Fault ('accident ouest-quercynois' according to Durand-Delga, 1979) is not as well known as the Villefranche fault. However, this fault constitutes the actual boundary between the Massif Central and the Aquitaine basin (Curnelle and Dubois, 1986) and corresponds to the 'discontinuité nord-aquitaine' (north Aquitanian fault) as defined by Autran et al. (1976). Although partly masked by the post-Oligocene cover, the West Quercy fault may be followed towards the north-west up to Perigueux (Durand-Delga, 1979; Gaillard and Masse, 1980) (Fig. 1). According to Gaillard and Masse (1980), this fault which trends NW–SE to NNW–SSE, bends near Perigueux and continues towards Rochefort with a N 130 E trend. However, the satellite imagery study (ERTS 1, LANSAT) shows that the West Quercy Fault remains with the same trend and continues as far as Nantes where it joins the South Armorican fault zone (Fig. 1). To the south-east, the satellite imagery and the morphological study show that the West Quercy fault crosses the western Montagne Noire where it constitutes one of the major faults in the pre-Hercynian basement (Saissac fault) and continues into the Carcassonne basin (Fig. 1). In the Hercynian basement, strike-slip offsets along the West Quercy fault are much smaller than those along the Villefranche fault (less than 1 km right-lateral offset may be inferred in the western Montagne Noire). This indicates that the development of the West Quercy fault was younger than that of the Villefranche fault and was originally a dip-slip fault of Late Carboniferous to Permian age. The marked difference in thickness of the Permian series shown by borehole data on either side of the West Quercy fault (Durand-Delga, 1979; Dauch, 1988) also supports this age estimate.

The Grésigne–Quercy area as studied in the present paper is arbitrarily limited to the north by the Lot valley, between Cahors and Figeac (Fig. 1). Data from a 3061 m deep well (GR1, COFEPA, 1960–1961) and a seismic section performed at the same time are available in the southernmost area. The well data are of high quality and core samples are still available. The seismic section does not have the accuracy of the modern seismic lines but the major reflections are rather well defined although not precisely identified.

On the whole, it appears thus that both the Villefranche and West Quercy faults are major regional basement faults on the scale of the French Massif Central and Aquitaine basin. On this scale, these faults intersect with no offset (Fig. 1) in spite of the deformation which occurred in the Grésigne–Quercy area.

2.2. Lithology and stratigraphy

2.2.1. The basement

On gravity survey maps (B.R.G.M. et al., 1974) the Grésigne block appears to have a 'heavy' basement which contrasts with the 'light' basement of the adjacent areas on both sides of the boundary faults. On the eastern side, this basement consists of various felsic gneisses with only occasional amphibolite layers or lenses (Rouergue–Levezou dome) and Upper Proterozoic to Lower Palaeozoic metasediments intruded by granitoid plutons (Albi–Decazeville area).

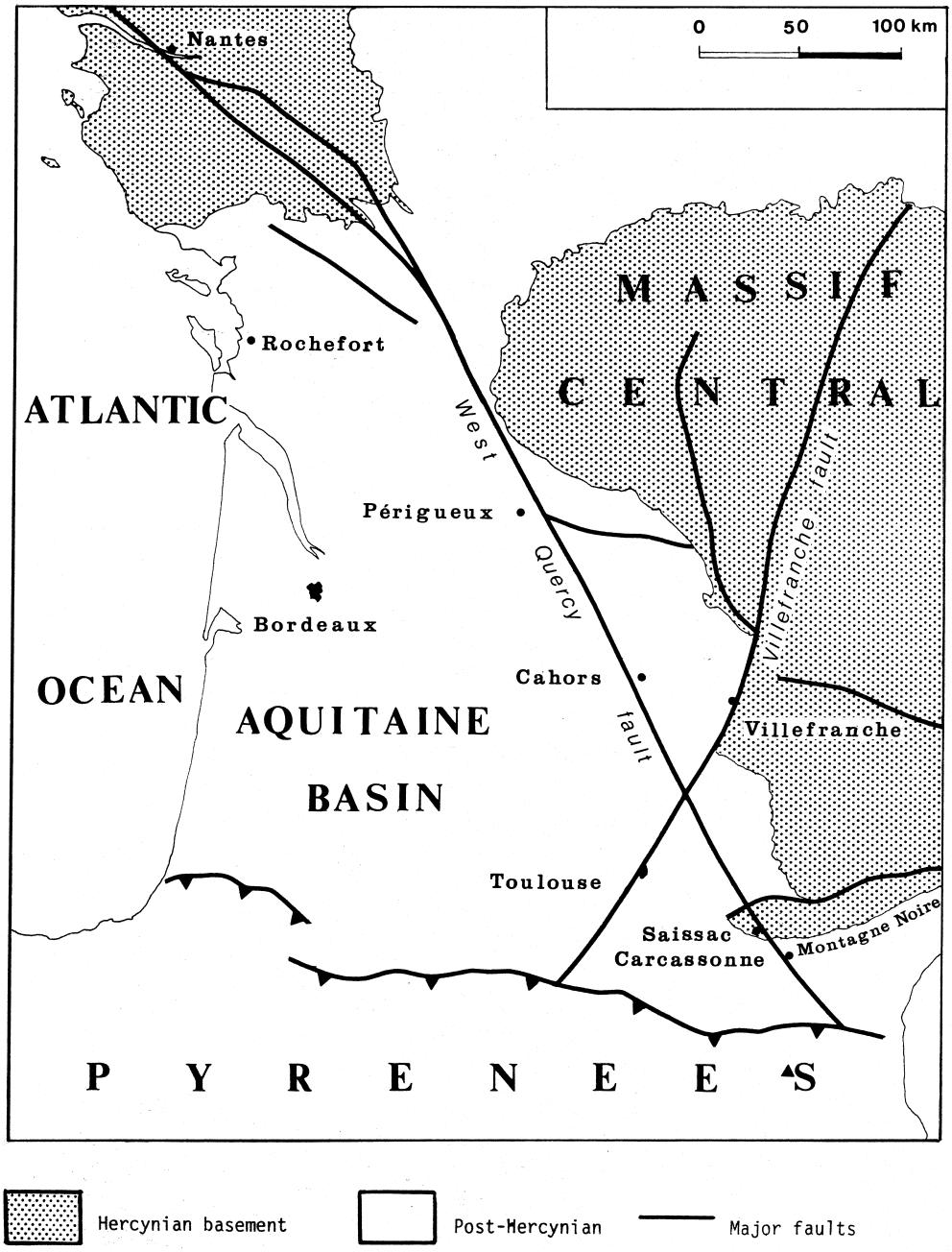

Fig. 1. Simplified geological map of the Grésigne–Quercy region. Late Carboniferous deposits are not represented.

On the western side, the basement was only accessed by drill-holes and was mapped using drill-hole data and gravity surveys (B.R.G.M. et al., 1974). This basement is constituted by Lower and Upper Palaeozoic sediments intruded by granitoid plutons which seem similar to those on the eastern side. If we consider the lithology of the southern Massif Central, it is likely that the greater density of the Grésigne basement is due to the presence of metasediments rich in biotite and other ferro-magnesian minerals including interbedded amphibolite layers. Studies of the deformation of the pre-Hercynian basement during the Alpine orogenesis in the nearby Pyrenees have shown that the overall ductility of the metasedimentary units was markedly greater than that of the granitoid-rich basement (e.g. Lamouroux et al., 1980; Soula et al., 1986).

2.2.2. The Late Carboniferous and Permian deposits

The Late Carboniferous and Permian deposits consist of continental conglomerates, sandstones and pelites unconformably overlying the Hercynian basement.

The Permian deposits are recognized under the Mesozoic and Cenozoic cover from well data through-

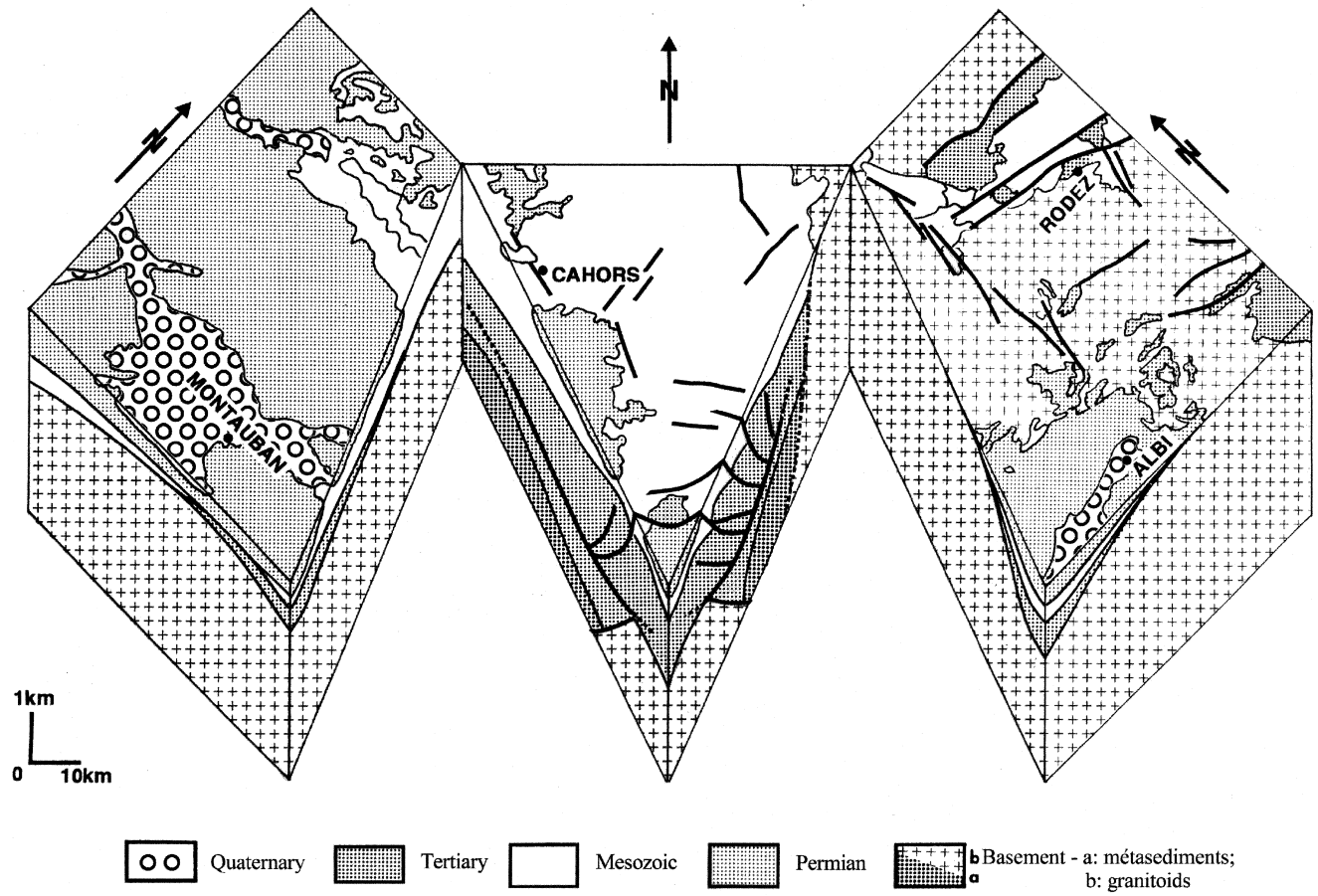

Fig. 2. Block-diagram of Grésigne–Quercy area.

out the studied region. They crop out within the Grésigne–Quercy block and outside it, near the southern tip of this block. A re-examination of the data presently available (Fabre, 1971; Delsahut, 1981) shows that these deposits are similar to those in the neighbouring Saint Affrique, Rodez and Lodeve Permian basins (Odin, 1986; Bourges, 1987; Rolando, 1988; Rolando et al., 1989).

The thickness of this series as observed in wells on both sides of the Grésigne block (0–700 m for the whole series) is consistent with that inferred in the Saint Affrique basin (0–1500 m, Legrand et al., 1994). However, the thickness as observed in the GR1 well in the southern Grésigne block is more than twice the maximum thickness of the corresponding series (the 'red' series) in the Saint Affrique basin. As discussed below, it is likely that this marked increase in thickness results from Alpine thrusting.

2.2.3. The Mesozoic deposits

The Mesozoic deposits consist primarly of Triassic pelites, sandstones and variegated marls (Carnian–Norian in age, 40 m thick) and Jurassic carbonates, predominantly limestones with interbedded marls and marly limestones (ca. 1000 m). A 50 m thick calcareous breccia (Upper Oxfordian in age) and a 50 m thick dolomitic interval (Portlandian in age) are observed at the upper part. The thickness of the Jurassic deposits varies slightly, and there is no noticeable difference between the Grésigne block and the surrounding areas.

Fig. 3 (*opposite*). Balanced cross-sections through apical region of the Grésigne–Quercy block. (a) Cross-section through Vaour dome (section A–A′ in Fig. 8). (b) Cross-section passing through GR1 well and intersection between the West Quercy and Villefranche faults (section B–B′ in Fig. 8). (c) Cross-section B–B′ after restoration. The sections are length-balanced. Data for cross-section (b) are from seismic section (line drawing after des Ligneris, 1961), field data and dip isogon maps, and GR1 borehole data (location of major faults after des Ligneris, 1961; Delsahut, 1981; Dauch, 1988 and bed dips after des Ligneris, 1961). Structure of basement and extensional faults under décollement are only speculative (no reflection in this area) and drawn on the basis of the geometry of the nearby Saint Affrique basin (Legrand et al., 1994). Ductile deformation of basement is assumed in restoration. Listric faults and roll-over structures speculated in cross-sections (b) and (c) are assumed to trend E–W as in Saint Affrique basin and are thus drawn as cross-cut by Villefranche fault in (c). Cross-sections (a) and (b) also show relationship between two conglomeratic sequences associated with South Grésigne and Saint Salvy thrusts. PF: Puycelsi fault; SGF: South Grésigne fault; AF: Abriols fault; VF: Vaour fault; SF: Soubirol fault. Numbers in circles indicate order of development of faults.

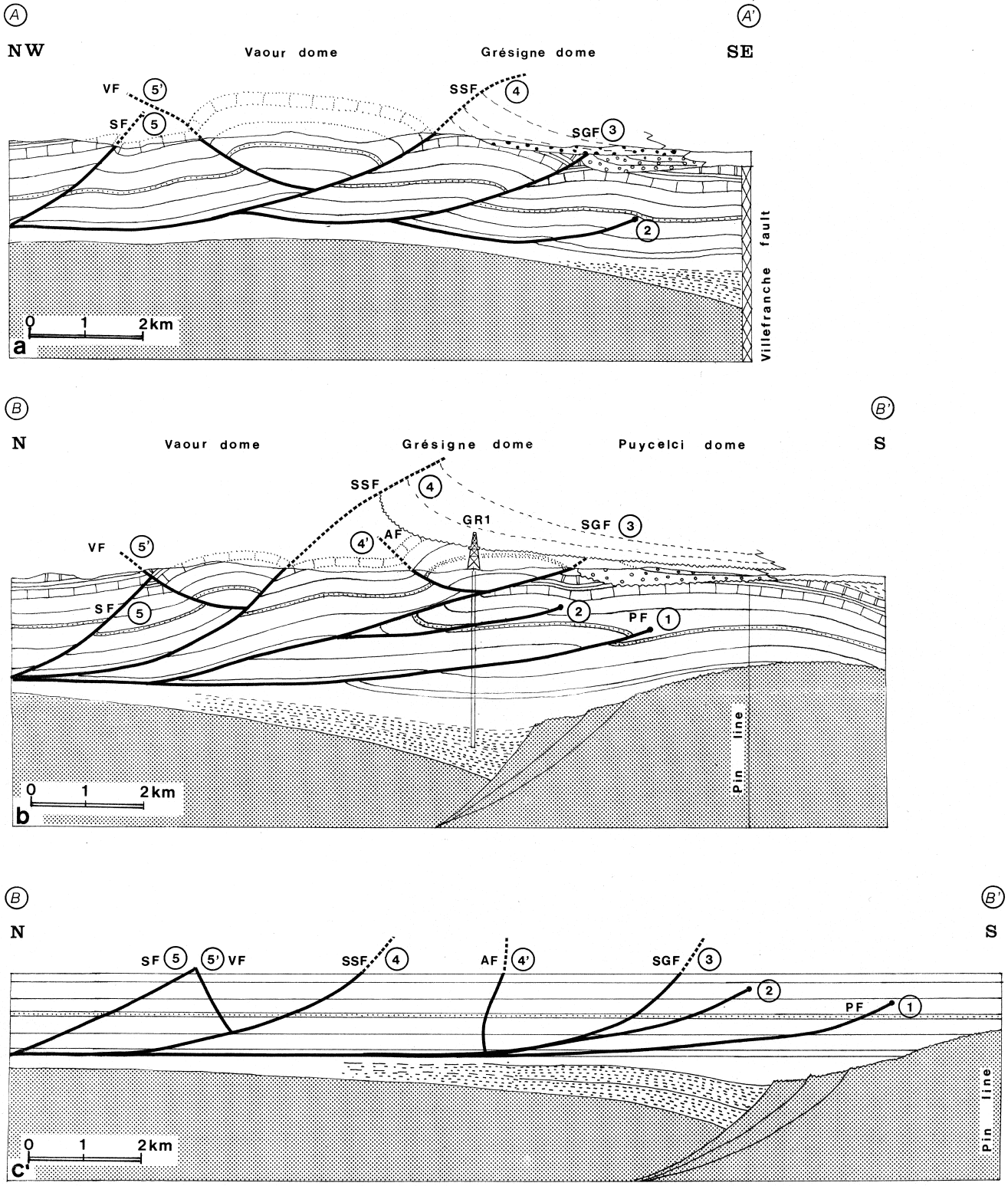
A
A'
NW
Vaour dome
Grésigne dome
SE
VF
5'
SF
5
SSF
4
SGF
3
2
Villefranche fault
0 1 2km
a
B
B'
N
Vaour dome
Grésigne dome
Puycelci dome
S
SSF
4
GR1
SGF
3
AF
4'
VF
5'
SF
5
2
PF
1
Pin line
0 1 2km
b
B
B'
N
S
SF
5
5'
VF
SSF
4
AF
4'
SGF
3
2
PF
1
Pin line
0 1 2km
c
Molasses d'Aquitaine
Grésigne conglomerates,upper sequence
Grésigne conglomerates, lower sequence
Dogger
Liassic marls
Liassic limestones
Upper Permian, red series
Lower Permian, grey series
Metasedimentary basement

Fig. 3.

Upper Cretaceous rocks are occasionally observed with a thickness that does not exceed 10 m. In the western part of the Grésigne–Quercy region, these Mesozoic deposits are cut by the West Quercy fault with vertical offsets of at most 100–200 m. The Mesozoic strata should be considered in this respect as a cover layer resting over a substrate consisting of the pre-Hercynian basement and Permian strata.

2.2.4. The Palaeogene deposits

Over most of the Aquitaine basin, the Palaeogene deposits are represented by the formation known as the Molasses d'Aquitaine. This formation consists of palustrine to fluviatile deposits with numerous intercalated palaeosoils.

The Palaeogene Grésigne conglomerates are observed only on the edge of the Grésigne block in front of the Grésigne thrust system. These conglomerates contain detritus from the footwall of this Grésigne thrust system including quartz from the Triassic sandstones and Jurassic limestone pebbles. The conglomerates pass westwards, eastwards, southwards, and upwards into the Aquitaine molasses (Viallard, 1985; Dauch, 1988; Paris et al., 1989). The upper part of this formation has been dated from fossil evidence as Early Oligocene (Muratet and Cavelier, 1992). It is likely that these conglomerates resulted from the development of the Grésigne thrust system and constitute the sedimentary infill of a localized foreland basin (Dauch and Viallard, 1987). The geometrical relationship between these conglomerates and the thrusts suggests that at least two depositional sequences occurred: the southernmost Puycelsi dome is unconformably covered by conglomerates (unit 1) which result from the earlier activity of the South Gresigne thrust (lower 'basin'-infilling sequence) and are then overriden by this thrust. The second conglomeratic unit (unit 2) rests over the South Grésigne thrust fault and is overriden by the Saint Salvy thrust sheet to the north. Unit 2 probably results from the earlier activity of the Saint Salvy thrust (upper 'basin'-infilling sequence) (Fig. 2).

2.3. Regional tectonic structures

The peculiarity of the Grésigne block is that it was much more deformed than the adjacent areas on both sides of the boundary faults during the Alpine regional shortening (Fig. 2). Three areas may be distinguished: the southern area which includes the Aveyron River drainage basin and corresponds to the apex of the block, the boundary fault zones and the northern area (Lot valley and Quercy region).

2.3.1. The southern area

The most characteristic structure in this area is a fold and thrust system which is thought to be responsible for a considerable increase in thickness of the Permian series (Fig. 3). At the surface, the strike of the thrust faults is E–W in the median part of the Grésigne block and NW–SE and NE–SW near the boundary faults. The curvature is especially marked in the case of the Grésigne and Saint Salvy thrust faults (Fig. 4). This means that these faults have a well-defined listric geometry in 3D representations (Fig. 4). The faults situated in the north of this area (Saint Antonin and La Grezié faults) maintain an E–W trend throughout the width of the wedge-shaped region except at the immediate contact with the boundary faults. These major thrusts are associated with regional scale domes which are located predominantly in the median and eastern parts of the block (Fig. 1). These domes were previously interpreted as resulting from cross-folding (Fournier, 1898; Gèze and Cavaillé, 1977) or basement uplift (Ellenberger, 1937; Durand-Delga, 1979). The Grésigne dome is the largest of these domes. On the map, it appears with a rounded shape. Dip isogons show that it is markedly asymmetrical and its crest line has, in fact, a curved trace which passes from E–W to NE–SW and is parallel to the trace of the South Grésigne thrust fault (Fig. 5). It is interpreted here as a triangular zone resulting from a fault-propagation fold related to an antithetic fault (Fig. 3). The curvature of the crest line of the dome is attributed to a faster transport near the axis of the wedge constituted by the Grésigne–Quercy block.

The Marnaves and Vaour domes (Fig. 6) also have a rounded shape with a less pronounced curvature of their crest lines. We interpreted them as thrust-propagation folds at the eastern tip of the Saint Salvy and Vaour thrust faults. The NW–SE trends of the inter-dome synforms and the analysis of minor fractures (see below) suggest, however, the occurrence of a superimposed NE–SW local shortening. To the south of the South Grésigne thrust fault, the Puycelsi dome (Fig. 1) is also interpreted as a fault-propagation fold (Fig. 3).

The relationship between the main thrusts and the Paleogene conglomerates enables us to establish the sequence of thrust propagation and shows that thrusting propagated northwards, i.e. backwards, with the successive development of the Puycelsi fault, the Grésigne fault and the Saint Salvy fault ('overstep' sequence) (Fig. 3).

2.3.2. The boundary fault zones

In the areas in immediate contact with the boundary faults, the regional structures are predominantly strike-slip faults parallel to the boundary faults and these areas may be considered as strike-slip fault zones. Pure strike-slip subvertical faults, however, are rather rare near the apex of the wedge-shaped block but are more numerous to the north. The directions and sense of

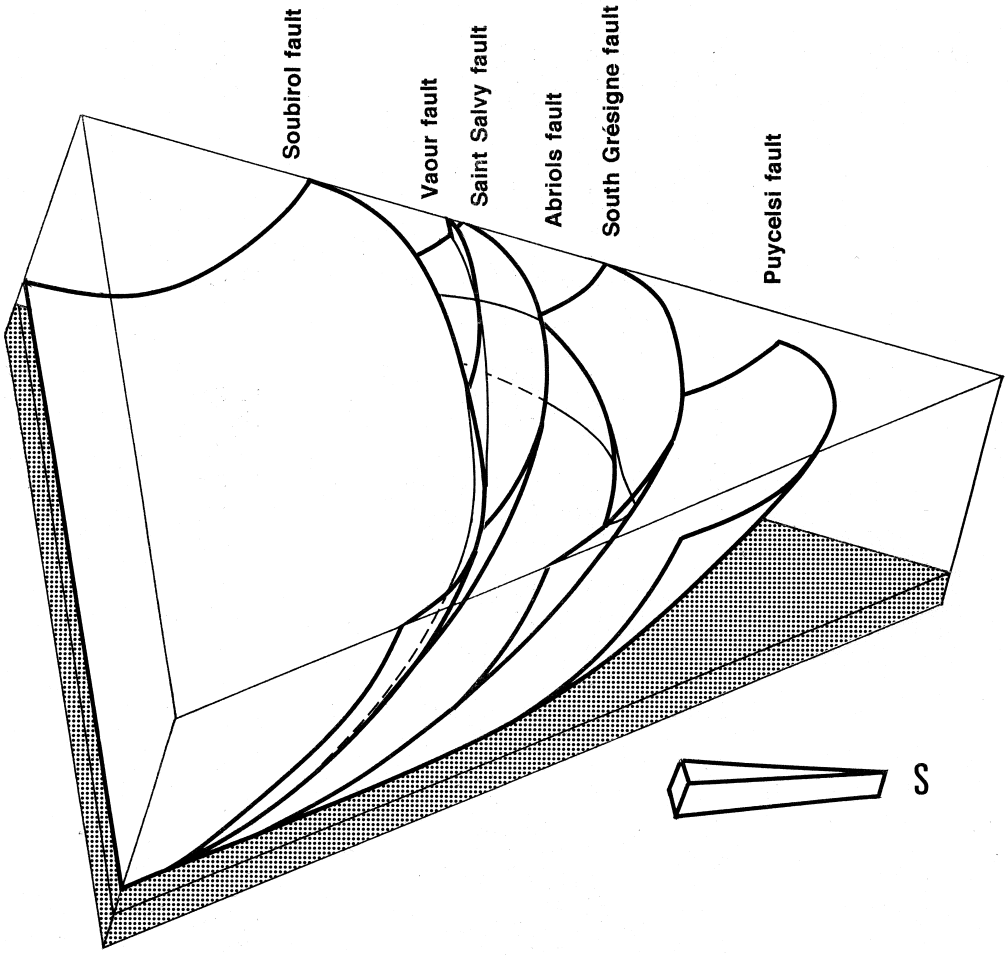

Fig. 4. 3D schematic representation of thrust faults in southern end of Grésigne–Quercy wedge-shaped block. The upper planar surface is approximately 300 m above sea level. The close-to-N–S vertical surfaces schematically represent the wedge-bounding regional strike-slip faults. For clarity, dips and curvatures of faults are accentuated.

displacement along the boundary faults are variable and are achieved at various times in the geological history.

The displacement along the Villefranche fault is well documented. Slip was mainly left-lateral from Late Carboniferous to Oligocene time (Grolier and Letourneur, 1968; Bergues et al., 1983; Muratet, 1983; Faure, 1995). When considering only middle Eocene to Oligocene events, left-lateral strike-slip offsets are of ca. 500–750 m as inferred from the relative displacement of the boundaries of the Maurs basin which is one of the Upper Eocene basins formed as en échelon pull-apart basins along the Villefranche fault zone (Muratet, 1983). The Maurs basin resulted from left-lateral wrenching of pre-existing oblique faults and other basins from left-stepping secondary left-lateral strike-slip faults (Muratet, 1983). Thus, it can be reasonably inferred that the sinistral relative displacement along the Villefranche fault zone was at least 1–2 km. This value is consistent with that inferred from the thrust structures of the southern area (3–4 km in the median part of the block) which formed at the same time. Dip-slip offsets are less than 100 m.

The displacements along the West Quercy Fault were right-lateral during Eocene to Oligocene time (Durand-Delga, 1979; Gaillard and Masse, 1980; Pélissié, 1982). The right-lateral displacement was inferred from microtectonic studies. The offsets could not be directly measured because of the absence of reliable markers. At 110 km to the northwest of the apex of the Grésigne–Quercy dome, a tight (limb dip of 50–75°) fold is observed in contact with the fault with an axial trace oriented 19° to the fault trace. This fold evolves into an open fold (limb dips $\leq 10°$) over a distance less than 1 km from the fault (Gaillard and Masse, 1980), suggesting that a ductile shear zone formed in the Mesozoic and Cenozoic cover as a precursor of the fault ('premonitary shear zone' according to Johnson, 1995). The variation in fold geometry near the fault can account for approximately 1 km of right-lateral displacement based on calculations that assume simple shear and (1) the fold axis represents the principal finite extension direction and (2) the fold geometry

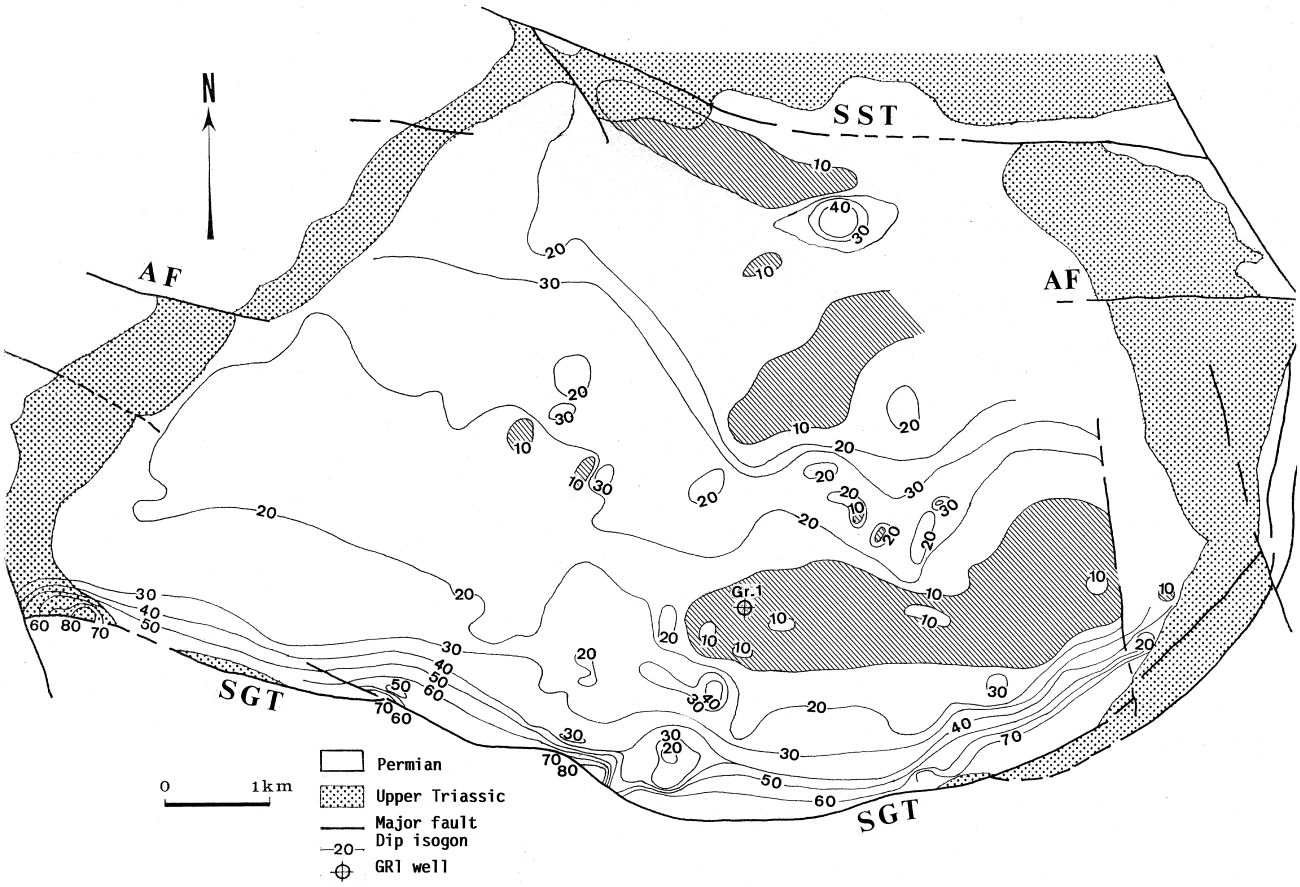

Fig. 5. Dip isogon map of the Grésigne dome (dip data from des Ligneris, 1961). Hatched areas have dip which is lower than 10°. Note rapid increase in dip when approaching South Grésigne Thrust and local dip variations near other thrust faults. SGT: South Grésigne Thrust, AF: Abriols fault, SST: Saint Salvy thrust.

reflects the magnitude of shortening. This displacement is significantly less than total right-lateral because it does not include fault slip. Therefore, the value of the right-lateral displacement along the West Quercy fault is of the same order of magnitude as that of the left-lateral displacement along the Villefranche fault. As in the case of the Villefranche fault, dip-slip offsets inferred from the cross-sections perpendicular to the West Quercy fault are one or two orders of magnitude smaller than the strike-slip displacements (10–200 m).

2.3.3. The northern area

In this area, the regional structures are predominantly strike-slip faults with NW–SE and NE–SW trends (Fig. 1). The NW–SE-trending faults show right-lateral slip and the NE–SW-trending faults left-lateral slip. Taken together, these observations show that these two fault sets can be considered to have acted as actual conjugate sets according to the definition of Johnson (1995). WNW–ESE- to ENE–WSW-trending reverse faults are present, but they are localized in the south and east of this area, at the contact with the Villefranche fault.

2.4. Minor structures

2.4.1. Minor folds

Fifty-one minor folds with half-wavelength between ca. 1 m and $n\times10$ m were analysed at 28 localities in the southern part of the block. The maximum shortening direction at each locality is assumed to be perpendicular to the axial plane and/or the axis of the folds (Fig. 6). The minor fold axis direction shows an arcuate trajectory parallel to the strike of the regional fold and thrusts which is consistent with a single folding episode. These data also confirm that the maximum shortening direction, which is N–S near the axis of the wedge diverges when approaching the boundary faults.

2.4.2. Minor fractures

Minor faults, extension fissures and stylolites were measured in 11 localities scattered within the Grésigne block and two localities outside. They were analysed using the treatment of Arthaud and Choukroune (1972) (Fig. 6) which assumes that the maximum shortening direction (assimilated to σ_1) bisects the minimum separation angle between the left-lateral and right-lateral strike-slip microfaults, and is parallel to

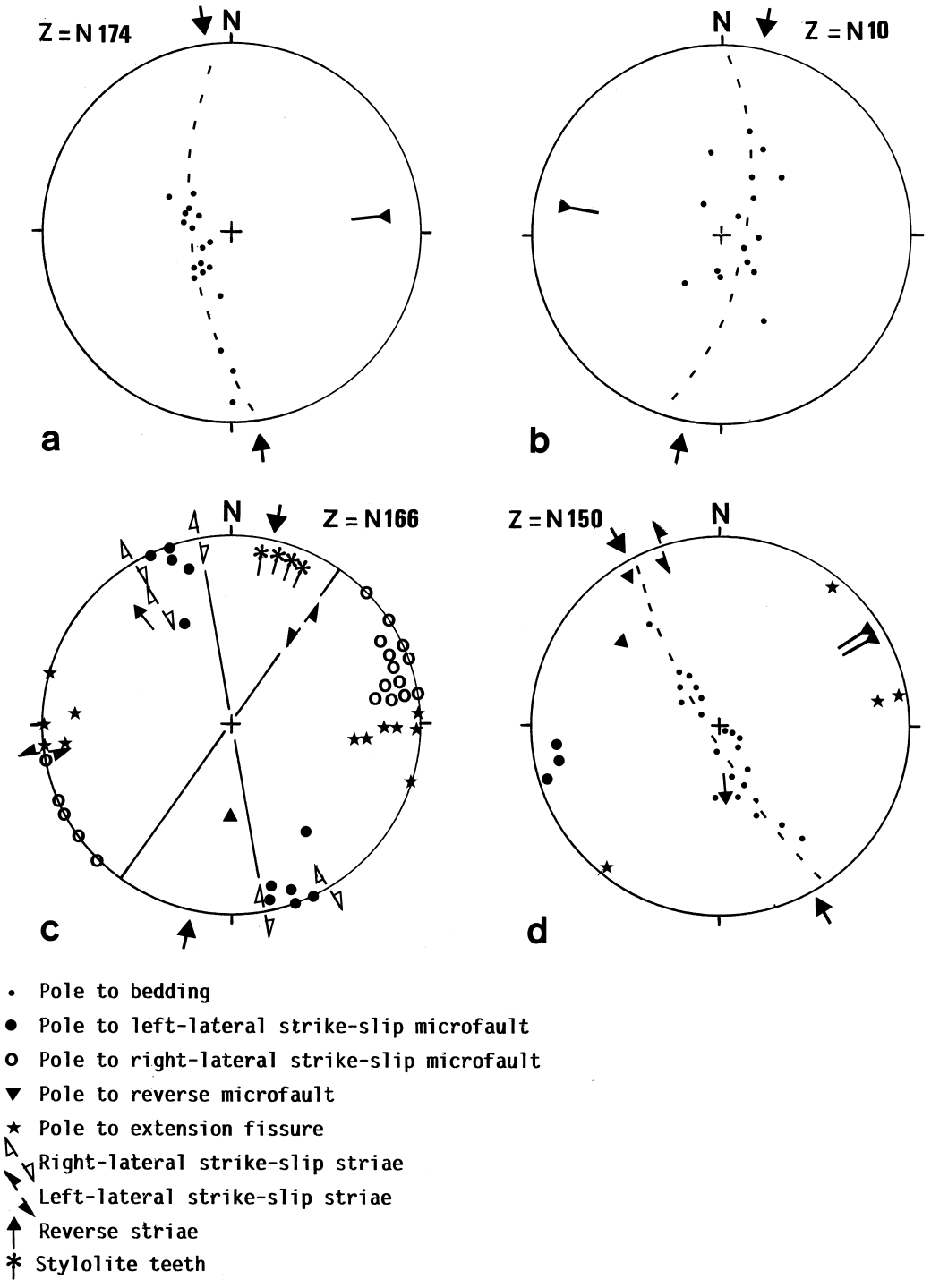

Fig. 6. Examples of microtectonic data used to infer maximum shortening directions. Projection into upper hemisphere. (a)–(d) Locations in Fig. 8. (a) Northern area, eastern side, (b) apical area, western side, northern contact of South Grésigne thrust, (c) northern area, western side, (d) northern area, eastern side.

the stylolite teeth and perpendicular to the extension fissures. This method was used here because of the variety in type of the structures available. The results reported in Fig. 7 show a maximum shortening direction which is consistent with that given by the minor folds: on the western side of the block, they are N5E–N20E; in the median part, they are close to N–S; in the eastern side, they are NNW–SSE. In two localities, an abnormal local shortening direction was found: NNE–SSW near Saint Antonin to the north and ENE–WSW near Saint Salvy, to the south-east. The latter shortening direction is similar to that inferred

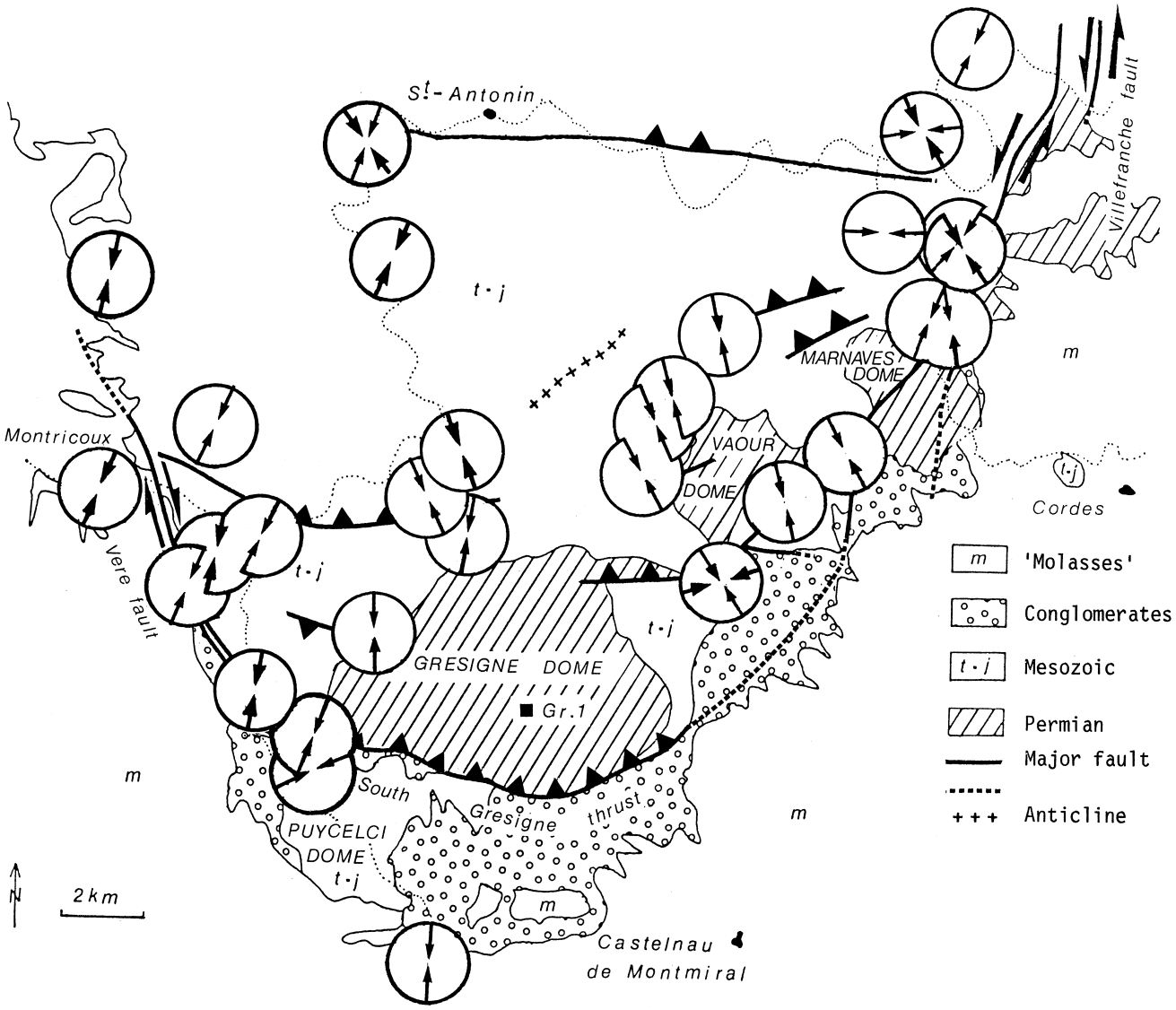

Fig. 7. Maximum shortening directions in the Grésigne–Quercy wedge-shaped block as inferred from minor fold and fault measurements (after Dauch, 1988). In stereograms, small arrows indicate microfold data and large arrows indicate microfault data.

from large-scale structures in the same area and is similarly interpreted as a second deformation episode related to a late transport parallel to the Villefranche fault.

2.5. Maximum shortening trajectories

The maximum shortening directions inferred from the minor structures are consistent with those shown by the regional scale structures (thrust and reverse faults, conjugate strike-slip faults and map-scale folds). Fig. 7 shows the maximum shortening trajectories constructed from both the minor structures (fractures and folds) and regional structures. These trajectories display a double concave pattern with a N–S mirror line passing through the centre of the Puycelsi dome.

In the northern area, near the Lot valley, the map-scale strike-slip faults form angles of close to 45° with the local maximum shortening directions which bisect the conjugate faults where they are present. In the southern area, the thrust and reverse faults belonging to the southern fold and thrust system are perpendicular to the maximum shortening trajectories (Fig. 8).

2.6. Structural interpretation

Fold and thrust structures in wrench systems (e.g. Bally, 1983; Harding, 1985) commonly display a geometry known as a 'flower structure'. The structures observed in the Grésigne–Quercy area differ markedly from the flower structures both in shape and displacement/strain patterns (see Richard and Cobbold, 1989) and they branch into a flat-lying décollement instead

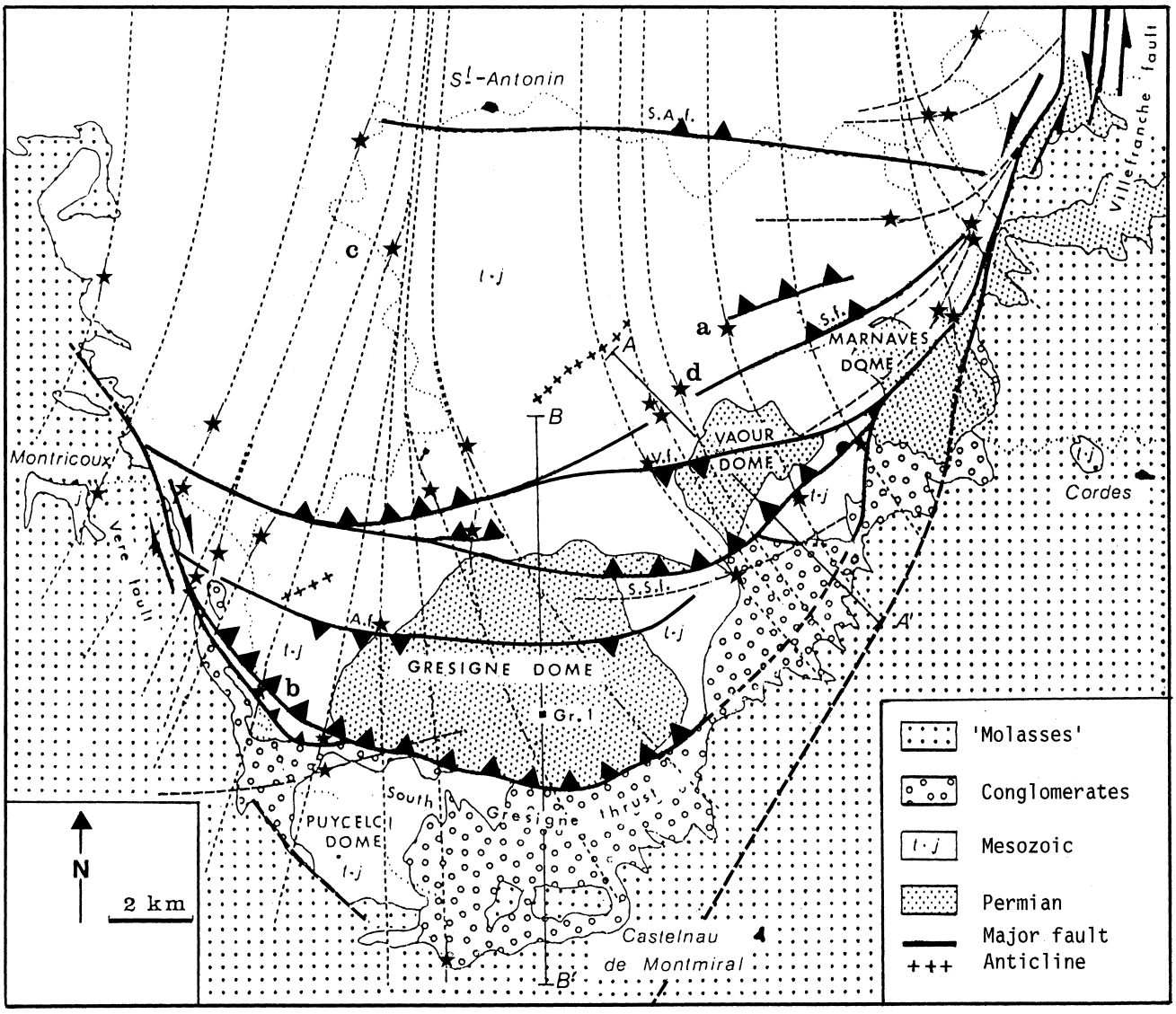

Fig. 8. Maximum shortening trajectories in the Grésigne–Quercy wedge-shaped block as inferred from minor and regional scale structures. A.f., Abriols fault; S.A.f., Saint Antonin fault; S.f., Soubirol fault; S.S.f., Saint Salvy fault; V.f., Vaour fault. A–A′ and B–B′ are traces of cross-sections shown in Fig. 2. Stars indicate microtectonic stations. (a)–(d) Locations of stereograms shown in Fig. 6.

of a vertical fault. At the immediate contact with the boundary faults, the fault pattern bears more resemblance to flower structures (e.g. Richard and Cobbold, 1989), but on the whole, the fold and thrust stuctures in the Grésigne–Quercy block are in fact similar to those found in thin-skinned fold and thrust belts.

The senses of displacement along the boundary faults and the sense of transport in the southern fold and thrust system combined with the shortening trajectories imply a motion of the entire block towards the south. The localized development of the fold and thrust system and the related crustal thickening and uplift near the intersection of the boundary faults strongly suggest that the movement was impeded in the corner made by the intersecting faults. The backwards ('overstep') propagation of the thrust system suggests a progressive tectonic accretion of material coming from the 'hinterland' against this 'locked up' zone as the wedge-shaped block moved southwards. In other words, it appears that the locked up zone propagated backwards with time.

2.7. Basement–cover relationship

The basement of the Grésigne–Quercy block is not accessible and no direct observation of the basement–cover relationship is possible. The basement and cover of the wedge-shaped block are both in contact with the surrounding rigid basement along major regional faults, requiring that bulk shortening was the same in the basement as in the cover. As shown above, strain proceeds essentially by thrusting and associated folding

in the cover but the décollement surface lies within the Permian series and not along the basement–cover interface. In view of the seismic section and GR1 well, it is rather unlikely that basement thrusts are connected to the structures seen in the cover. In any event, other mechanisms are capable to have deformed this basement which is highly anisotropic. In the nearby Pyrenees, a similar metasedimentary basement has been shown to have deformed in a ductile manner during the Alpine orogenesis with development of new (Alpine) foliations and reactivation of older (Hercynian) foliations (Lamouroux et al., 1980). A ductile deformation of the basement in the Grésigne block is less troublesome when we consider that the overall regional shortening is not here as large as in the Pyrenees. It was at most −14 to −18% if the 3–4 km shortening inferred in the cover of the apical region was the same in the basement underneath. It seems likely that the thrust faults and associated detachments developed successively in the cover as strain increased in the basement. The northern end of the basal detachment (situated outside the section shown in Fig. 2) is likely to represent the limit beyond which strain could be neglected both in the basement and the cover.

3. Part II—comparison with Prandtl–Nadai cell

Analogy has often been drawn between plane strain plastic flow and tectonic processes (Odé, 1960; Varnes, 1962; Johnson, 1970; Tapponnier and Molnar, 1976; Molnar and Tapponnier, 1977, amongst others). The material is assumed to be perfectly plastic, with no volume change and no strain hardening. In plane strain, the two common yielding criteria (Tresca's and von Mises') are equivalent: plastic flow occurs when the maximum shear stress, $\tau = (\sigma_1 - \sigma_3)/2$, becomes equal in value to the yield stress k (σ_1 and σ_3 are the maximum and minimum stress, respectively). In this case, the maximum shear stress trajectories coincide with slip lines, i.e. are at 45° to the stress principal direction (Nadai, 1950, p. 547). Slip or shear strain occurs parallel to the slip lines, α slip lines in the case of right-lateral shear sense and β slip lines in the case of left-lateral shear sense. In the case of geological structures, these slip line trajectories represent the directions along which real faults can occur.

In Prandtl's original plane strain compressed cell (1924) a perfectly plastic mass is confined between two very long, approaching, parallel, rigid and perfectly rough plates such that the shear stress τ along the plates reaches the yield stress k; the material is permitted to extrude in one direction only and the plates squeezing the material remain parallel to one another. The slip lines are represented by two systems of cycloids which cross one another at right angles. The contact between the two plates and the mass are natural limits of the plastic region and are at the same time envelopes of the slip lines (Hill, 1950; Nadai, 1950; Freudenthal and Geringer, 1958; Kanizay, 1962).

Nadai (1950, p. 542) has shown that the solution for the compressed cell of Prandtl is related to the solution of a compressed wedge-shaped cell where the only difference in the boundary conditions is the angle between the plates: for Prandtl's conditions it is 0°, for Nadai's cell the angle may range from 0° to 180°. Nadai's solution for the wedge-shaped cell assumed movement of material out of the constricted end of the cell (Fig. 8a). In order to interpret converging faults in the western part of the South Silverton district (Colorado), Varnes (1962) gives a similar solution for a compressed wedge-shaped cell where the material moves out of the cell towards the open end (Fig. 8b). The slip lines for the wedge-shaped cell solutions are exponential curves rather than cycloids. Both Nadai's and Varnes' solutions are termed 'passive case' because the mass being extruded is said to passively respond to pressure exerted by the plates and the slip lines are concave towards the direction of movement of material.

In the active case, a push on the material from one end in the direction of movement causes the mass to actively press on the plates and moves them outwards and at the same time extrudes the material forwards. Under these circumstances, the slip lines are convex towards the direction of movement of the material. Where this direction is towards the constricted end of the cell (Fig. 9c), the slip lines have the same geometry as Varnes' passive case but the movement of material is in the opposite sense (Kanizay, 1962).

The tectonic structures in the Grésigne wedge-shaped block are consistent with the slip line field computed for the active case of a wedge-shaped cell, with material moving towards the apex (Figs. 9c and 10). To avoid confusion in the following section, the computed active case wedge-shaped cell will be referred to as the 'theoretical cell' and the natural example as the Grésigne–Quercy wedge-shaped block.

3.1. Similarities and differences between the Grésigne–Quercy wedge-shaped block and the Prandtl–Nadai theoretical model

On the whole, the observations reported in Part I show good agreement between the natural example and the theoretical model in terms of geometry, kinematics, rheology, strain conditions and stress trajectories. Deviations from the model predictions are observed, however, in certain parts of the natural wedge-shaped block. The similarities and differences are described below.

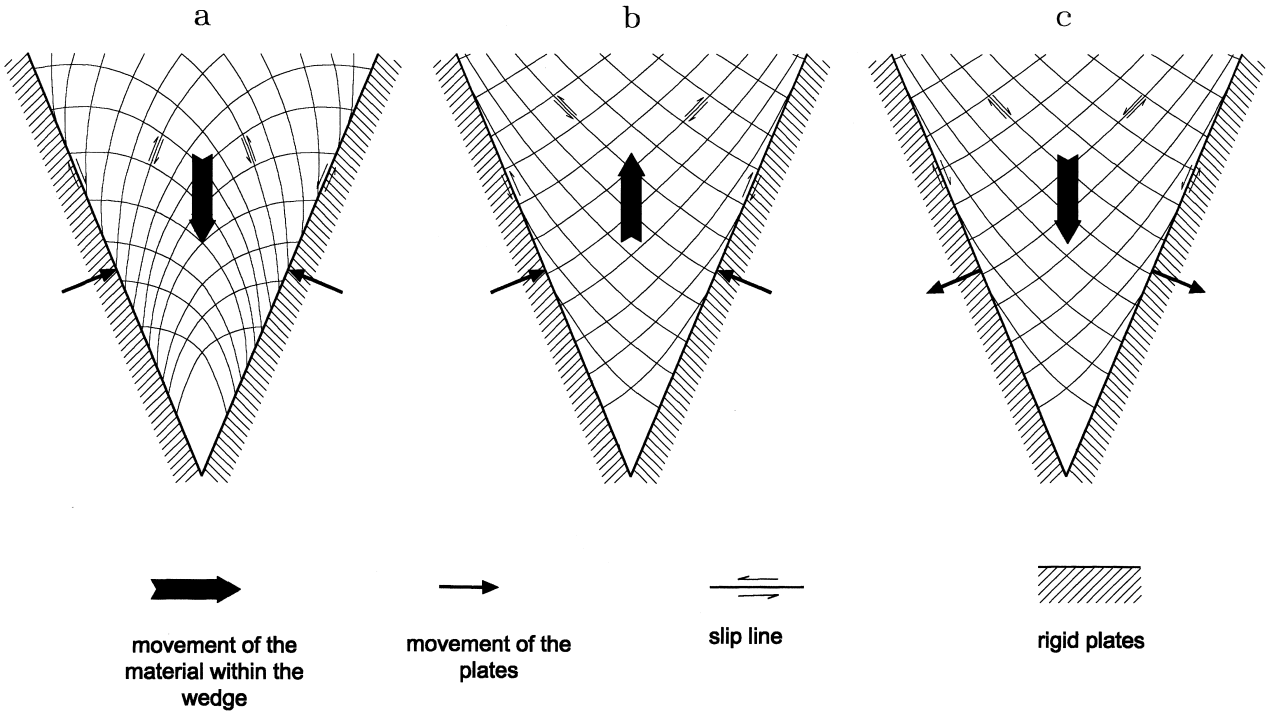

Fig. 9. Slip-line field in a wedge-shaped cell. (a) Passive case with movement of material out of constricted end of wedge (after Nadai, 1950, fig. 37-17, p. 542), (b) passive case with movement of material towards open end of wedge (after Varnes, 1962, fig. 19), (c) active case with movement of material out of constricted end of wedge (after Kanizay, 1962, fig. 8c).

3.1.1. Rheology

During Alpine deformation, the granitoid-rich undeformed basement of the plates (outside the wedge-shaped block) can be considered as rigid when compared with the deformed Permian and Mesozoic deposits and their granitoid-free metasedimentary basement. Even though stress may vary with time, the regional stress–strain curve of such geological materials would resemble that of a perfectly rigid-plastic material when averaged over a long period of time (Varnes, 1962; Tapponnier and Molnar, 1976). Therefore, the assumption of rigid-plasticity and constant-volume deformation seems reasonable in the case of the Grésigne–Quercy cell. The Villefranche and West Quercy faults can be considered as the boundaries between the rigid-plastic medium and the rigid plates.

3.1.2. Geometry and kinematics

The angle of opening of the Grésigne–Quercy block is approximately 45° and its radius 60 km. The axis strikes N–S and the apex is situated at the south. The material moved southwards, from the large end to the apex, as a result of Alpine regional shortening and the material outside the cell remained undeformed. These geometrical characteristics are similar to those in the model but the natural example differs from the model in two respects. First, in the theoretical cell, the material is forced to flow out of the constricted end of the wedge-shaped cell, whereas in the Grésigne–Quercy cell, the apex is considered to be closed. Second, the boundaries move apart in the theoretical cell whereas they remain immovable in the Grésigne–Quercy cell. As a consequence, the material near the apex has moved upwards normal to the plane of the cell.

3.1.3. Strain conditions

A plane horizontal strain analysis is justified for most of the Grésigne–Quercy block (northern area) since here the largest displacements are horizontal movements along strike-slip faults. Plane horizontal strain analysis is not possible, however, in the southern area where a noticeable crustal thickening occurred as a result of thrusting. This discrepancy with the theoretical model seems to be due to the immovability of the plates and the closure of the apex.

3.1.4. Stress trajectories and structural patterns

In the theoretical cell, the σ_1 and σ_3 trajectories in the horizontal plane bisect the right angle between the slip lines. Along and near the bisectrix of the theoretical cell, σ_1 and σ_3 are oriented parallel and perpendicular to this bisectrix (Fig. 11). The principal stress trajectories rotate sideways so that they meet the boundaries at an angle of 45°. Consequently, σ_1 trajectories diverge symmetrically with respect to the axis, towards the south-west in the western side and towards the south-east in the eastern side. Concurrently, σ_3

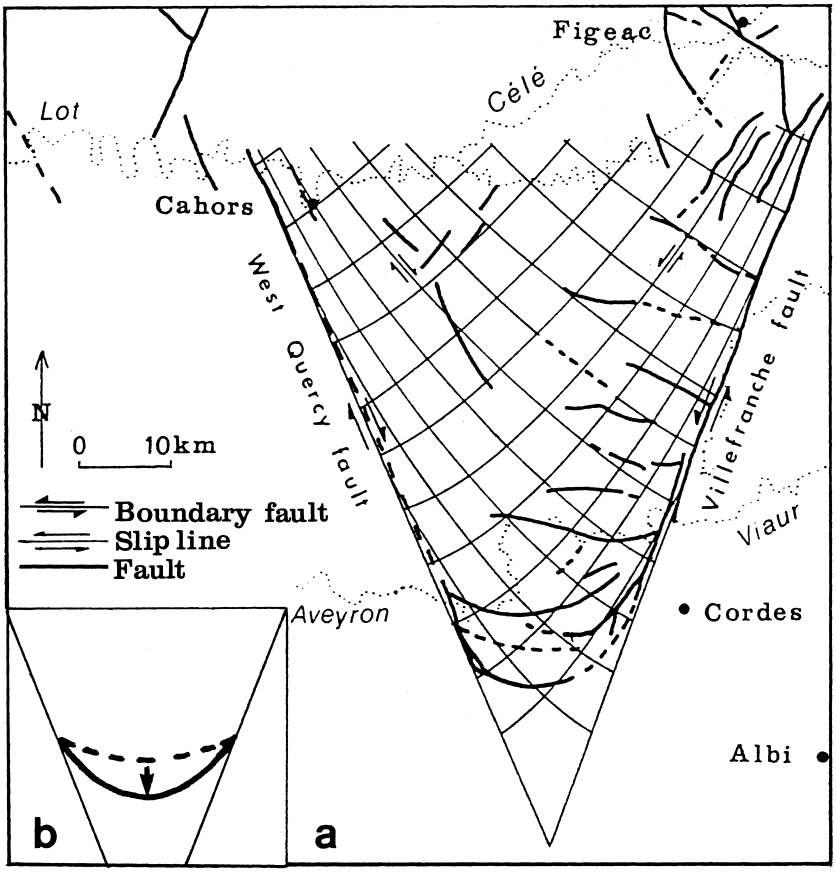

Fig. 10. (a) Comparison between fault network in Grésigne–Quercy wedge-shaped block and slip-line field in wedge-shaped Prandtl–Nadai cell. (b) Traces of South Grésigne thrust fault before and after restoration using balanced section in Fig. 2. Interrupted line represents initial trace and arrow shows displacement as a result of finite strain.

trajectories are broadly oriented perpendicular to the axis of the wedge-shaped block and show an arcuate pattern concave towards the wide end.

In the northern part of the Grésigne wedge-shaped block, the structural pattern agrees well with the model. The direction and slip sense of the strike-slip faults are similar to those of the slip lines predicted by the model: there are strike-slip faults displaying NNW–SSE to NW–SE trends with right-lateral slip and NNE–SSW to NE–SW trends with left-lateral slip. It is worth mentioning that these strike-slip faults match the predictions of a perfectly plastic material (orientations at nearly 45° to the stress principal directions) rather than the predictions of a Mohr–Coulomb model. The maximum shortening trajectories are similar in direction to those of σ_1 in the model, although the pattern is less symmetric than the model.

At the southern end of the Grésigne–Quercy block, the maximum shortening trajectories remain similar to those in the model (compare Figs. 8 and 11). The fault pattern, however, differs markedly. The main faults here are dip-slip reverse (thrust) faults and their trace is broadly perpendicular to the maximum shortening trajectories and thus parallel to the trajectories of the minimum principal stress predicted by the model. The parallelism is almost perfect in the case of the faults situated in the north of this area (Abriols, Saint Salvy and Vaour faults), except near their junction with the boundary faults. The curvature is more accentuated in the case of the Grésigne frontal thrust.

3.2. Interpretation

The essential difference between the model and the natural wedge-shaped cell lies in the fact that in the natural wedge-shaped cell, the apex is closed and the plates immovable so that the material in the apical zone is not forced to flow between plates that move apart, as in the model, but is locked up and pushed forwards (and sideways) against the immovable plates acting as a 'closed gate'. This results in a local increase in the horizontal principal stresses σ_1 and σ_3, whereas the vertical stress, which is equal in value to the lithostatic stress σ_z, remains unchanged at a given depth. As long as σ_3 is less than σ_z, plane horizontal strain occurs through strike-slip faulting as is observed in the northern portion of the Grésigne–Quercy block (Fig. 11, top). In the apical zone, when the horizontal

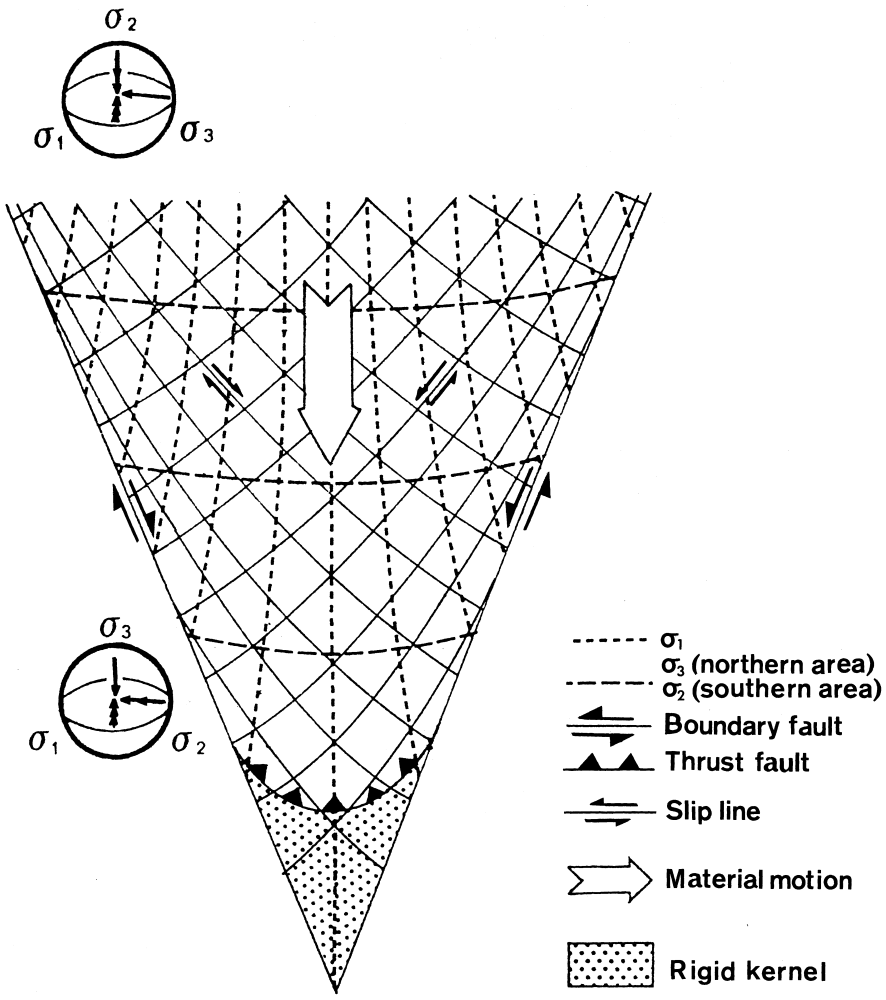

Fig. 11. Interpretation of Paleogene deformation in the Grésigne–Quercy wedge-shaped block using proposed modified cell model. Insets show disposition of principal stress axes in northern (top) and southern (bottom) areas.

stress values are especially high, the horizontal stress perpendicular to σ_1 will become the intermediate principal stress (σ_{2ap}) and σ_z the minimum principal stress (σ_{3ap}). σ_1 and σ_3 lie in the vertical plane parallel to the direction of σ_1 (Fig. 11, bottom). As a result, deformation is accomplished by thrust faulting and crustal thickening occurs. The sequence of thrust propagation in the southern portion of the Grésigne–Quercy block confirms that locking up was initiated near the apex and then propagated towards the wide end.

The directions of the principal stress axes in the Grésigne–Quercy cell are the same as in the theoretical model. The maximum principal stress σ_1 increases in value in the apical zone but it does not change its direction. One of the two other principal stresses is vertical everywhere. In the northern part of the Gresigne cell, this vertical stress is σ_2 as in the theoretical cell. In the southern part where the material is blocked, this vertical stress is σ_3. As a consequence, the σ_2 trajectories will be the same as those of σ_3 in the theoretical cell and will meet the boundary faults at an angle of 45°. The unstrained, or poorly deformed area at the end of the apical zone could be analogous to the rigid kernel ('dead zone') developed at the contact of a rigid plate squeezing a plastic mass (Nadai, 1950; Freudenthal and Geringer, 1958) (Fig. 11).

In the modified theoretical model we propose in the present paper, the thrust faults which are assumed to strike parallel to the direction of σ_2, meet the boundary faults at an angle of 45°. In the apical zone of the Grésigne cell, the thrust faults which are observed in the Mesozoic cover meet the Villefranche and West Quercy faults tangentially. Therefore, the strike-slip faults in this Mesozoic cover may have followed precursor ('premonitary' after Johnson, 1995) shear zones (S. Wojtal, written suggestion). The Mesozoic cover can be considered in this respect as a cover layer in which a shear zone evolving into a fault developed as a result of the reactivation of a basement fault (or fault zone). This may explain why the curvature of the trace of the thrust faults becomes more accentuated when approaching the apex (e.g. the Grésigne thrust)

where the fault contact zones occupy a relatively large proportion of the width of the wedge-shaped block. The net displacement inferred from the measured deflection of the thrust conforms with the inferred net southwards transport of the back of the block (Fig. 10b). Further evidence for the reactivation of basement faults could be found in the fact that a component of strike-slip is added to the dip-slip component on the thrust fault surfaces when approaching the boundary faults and, conversely, that a component of dip-slip reverse motion is observed along the boundary faults, especially on both sides of the apical zone.

4. Conclusion

The Grésigne–Quercy area provides a record of the deformation occurring within the acute angle of two intersecting regional strike-slip faults. As in many other natural examples, the shear sense along these regional strike-slip faults indicate a maximum regional shortening direction which bisects the acute angle formed by these faults. They can thus be considered to have acted as conjugate faults as defined by Johnson (1995). The direction of regional maximum shortening is here confirmed from microstructural evidence.

The variation of the Prandtl–Nadai theoretical model used here (active case with material moving towards the apex between immovable rigid plates) gives a satisfactory explanation for the structural pattern of the Grésigne–Quercy area. The principal—and most spectacular—result is the development of a south-verging thrust and fold system near the junction of the faults. The fold and thrust structures in the Grésigne–Quercy area are similar to those found in thin skinned fold and thrust belts and do not have 'flower structure' geometry more typical of strike-slip systems. The backwards propagation of the thrusts can be considered as evidence that the southwards moving material within the wedge-shaped region between faults was blocked in the corner formed by the intersecting faults.

Can this model be applied to other similar fault junctions where the regional shortening direction lies in the acute angle of the intersecting faults? Other models of fault intersections require either a sequential development of intersecting faults with mutual offsets which imply a widening of the intersection area (Horsfield, 1980; Ramsay and Huber, 1987, pp. 514–515; Lamouroux et al., 1991) or a rotation of the faults towards the plane perpendicular to the maximum shortening direction as the material within and outside the wedge-shaped block deforms in a ductile manner (Odonne and Massonnat, 1992). No such structural patterns have been observed in the Grésigne area. The model we propose in the present paper may explain why displacements occurred along the intersecting faults even though there was no offset, no widening of the intersection area and no rotation of these faults in the intersection area. It shows also that a strain localization may occur in the apex of the wedge-shaped block whereas the faults remain with the same position and the material outside the wedge-shaped block undeformed.

The analogy between the Grésigne–Quercy area and the modified Prandtl–Nadai model requires special geometric, kinematic, rheologic and strain conditions. The kinematic, geometric and strain conditions are observed in many regional examples. The rheological condition, however, seems to be not so frequently satisfied. In the Grésigne–Quercy area, the lower strength of the wedge-shaped block as a whole is essentially ascribed to the lower strength of the basement. This is not necessarily the same in other examples because intersecting regional strike-slip faults do not necessarily isolate a more ductile part of the basement within their acute angle. Other factors, however, might have been responsible for a ductile behaviour of such a wedge-shaped block defined by the acute angle of intersecting faults. One of these factors could have been, for example, the presence of multiple and variously oriented pre-existing faults or foliation planes. It is also suggested that strain softening processes could also have preferentially occurred in such blocks defined by faults at low angle to the maximum compressive stress direction. These latter points need further consideration but this suggests that models derived from the active case Prandtl–Nadai cell model might be of general interest in fault intersection problems.

Acknowledgements

M. Durand-Delga and R. Curnelle are thanked for stimulating discussions during various stages of the study. D.M. Fisher, S. Wojtal and G. Batt improved greatly the content and writing of the manuscript.

References

Anderson, E.M., 1951. The Dynamics of Faulting. Oliver & Boyd, Edinburgh.

Autran, A., Gérard, A., Weber, C., 1976. La carte gravimétrique de la France. Exemples d'utilisation géologique. Bulletin de la Société Géologique de France XVIII (7), 1119–1132.

Arthaud, F., Choukroune, P., 1972. Méthode d'analyse de la tectonique cassante à l'aide de microstuctures dans les zones peu déformées. Revue Institut français du Petrole XXVII (5), 715–732.

Bally, A.W., 1983. Seismic expression of structural styles. A picture and work atlas. American Association of Petroleum Geologists series 15, vol. 3, part 4 (strike-slip tectonics).

Bergues, P., Grolier, J., Soula, J.-C., Travert, P., 1983. Interprétation de la structure du bassin houiller de Saint-Eloy d'après les résultats d'essais mécaniques et les modèles tectoniques. Proceedings of the 5th Congress of the International Society for Rock Mechanics, Melbourne (Australia).

Bourges, Ph., 1987. Sédimentation alluviale et tectonique extensive dans le permien du Détroit de Rodez (Aveyron, France). Thèse Université Toulouse III, 186 pp.

B.R.G.M., ELF-R.E., ESSO-R.E.P., S.N.P.A., 1974. Géologie du bassin d'Aquitaine. Edited by Bureau de Recherches Géologiques et Minières, Orléans (France), 28 pp.

Curnelle, R., Dubois, P., 1986. Evolution mésozoique des grands bassins sédimentaires français; bassin de Paris, d'Aquitaine et du sud-est. Bulletin de la Société Géologique de France II (4), 529–546.

Dauch, C., 1988. Décrochements et chevauchements dans une zone de plate-forme: l'exemple du massif de la Grésigne (Aquitaine nord-orientale). Thèse Université Toulouse III, 171 pp.

Dauch, C., Viallard, P., 1987. Stade initial d'un duplex dans une aire à faible taux de raccourcissement: interprétation du pli chevauchant de la Grésigne (SW de la France). Comptes Rendus de l'Académie des Sciences de Paris 304 (II), 663–668.

Dauch, C., Inglès, J., Viallard, P., 1989. Modèle de déformation d'un coin crustal dans une zone de plate-forme: exemple du bloc Quercy–Grésigne (Aquitaine orientale, SW de la France). Comptes Rendus de l'Académie des Sciences de Paris 308 (II), 1017–1023.

Delsahut, B., 1981. Dynamique du bassin de Carmaux et géologie du Stéphano-Permien des environs (entre Réalmont et Najac). Thèse 3ème Cycle, Toulouse III, 232 pp.

Durand-Delga, M., 1979. L'Anticlinal de la Grésigne (Tarn, Haut-Languedoc), résultat du coulissement d'un bloc crustal quercynois. Comptes Rendus de l'Académie des Sciences de Paris 289 (D), 9–12.

Ellenberger, F., 1937. Recherches tectoniques sur le massif de la Grésigne. Bulletin de la Société d'histoire naturelle de Toulouse 71, 195–246.

Fabre, J., 1971. Contribution à l'étude du massif de la Grésigne. Thèse 3ème Cycle, Université Paris VI, 138 pp.

Faure, M., 1995. Late orogenic carboniferous extensions in the Variscan French Massif Central. Tectonics 14, 132–153.

Fournier, E., 1898. Le dôme de la Grésigne (Feuille de Montauban). Bulletin du Service Géologique de la France 66, 331–339.

Freudenthal, A.M., Geringer, H., 1958. The mathematical theories of the inelastic continuum. Handbuch der Physic; elasticity and plasticity, VI, pp. 229–433.

Gaillard, M., Masse, P., 1980. Un modèle de tectonique de plate-forme: exemple d'un linéament de la bordure nord-aquitaine. Bulletin des Centres de Recherches Exploration–Production Elf Aquitaine 4, 633–647.

Gèze, B., Cavaillé, A., 1977. Aquitaine orientale. Guides Géologiques Régionaux. Masson, Paris, 184 pp.

Grolier, J., Letourneur, J., 1968. L'évolution tectonique du grand Sillon Houiller du Massif Central français. Proceedings of the 23rd International Geological Congress 1, 107–116.

Harding, T.P., 1985. Seismic characteristics and identification of negative flower structures, positive flower structures, and positive structural inversion. American Association of Petroleum Geologists. Bulletin 69, 582–600.

Hill, R., 1950. The Mathematical Theory of Plasticity. Clarenden Press, Oxford, 356 pp.

Horsfield, W.R., 1980. Contemporaneous movement along crossing conjugate normal faults. Journal of Structural Geology 3, 305–310.

Johnson, A.M., 1970. Physical Processes in Geology. Freeman, Cooper & Co., San Francisco, California, 577 pp.

Johnson, A.M., 1995. Orientations of faults determined by premonitary shear zones. Tectonophysics 247, 161–238.

Kanizay, S.P., 1962. Mohr's theory of strength and Prandtl's compressed cell in relation to vertical tectonics. U.S. Geological Survey Professional Paper, 414 B, 16 pp.

Lamouroux, C., Soula, J.C., Déramond, J., Debat, P., 1980. Shear zones in the granodioritic massifs of the Central Pyrenees and the behaviour of these massifs during the Alpine orogenesis. Journal of Structural Geology 2, 49–53.

Lamouroux, C., Inglès, J., Debat, P., 1991. Conjugate ductile shear zones. Tectonophysics 185, 309–323.

Legrand, X., Soula, J.-C., Rolando, J.-P., 1994. The Saint-Affrique Permian basin (southern France): an example of a roll-over controlled alluvial sedimentation during regional extensional tectonics. Geodinamica Acta 7, 103–120.

des Ligneris, G., 1961. Rapport géologique de fin de sondage La Grésigne n°1 (GR1), C.O.F.E.P.A., Dt Exploration, unpublished (Bureau de Recherches Géologiques et Minières, France, ref. 931-4-1).

Molnar, P., Tapponnier, P., 1977. Relation of the tectonics of eastern China to the India–Eurasia collision: application of slip-line field theory to large-scale continental tectonics. Geology 5, 212–216.

Muratet, B., 1983. Géodynamique du Paléogène continental en Quercy-Rouergue. Analyse de la sédimentation polycyclique des bassins d'Asprières (Aveyron), Maurs (Cantal) et Varen (Tarn-et-Garonne). Thèse 3ème Cycle, Université de Toulouse, 188 pp.

Muratet, B., Cavelier, C., 1992. Caractère séquentiel discontinu des molasses oligocènes à la bordure orientale du Bassin aquitain; signification des conglomérats bordiers (Tarn, Tarn-et-Garonne, sud-ouest de la France). Géologie de la France 1, 3–14.

Nadai, A., 1950. Theory of Fracture and Flow of Solids. McGraw-Hill, New York, 572 pp.

Odé, H., 1960. Faulting as a velocity discontinuity in plastic deformation. In: Griggs, D.T., Handin, J. (Eds.), Rock Deformation Symposium. Geological Society of America Memoirs 79, pp. 293–321.

Odin, B., 1986. Les formations permiennes, Autunien superieur à Thuringien du 'bassin' de Lodève (Hérault, France): stratigraphie, minéralogie, paléoenvironnements, corrélations. Thèse Université Aix-Marseille III, 329 pp.

Odonne, F., Massonnat, G., 1992. Volume loss and deformation around conjugate fractures: comparison between a natural example and analogue experiments. Journal of Structural Geology 14, 963–972.

Oertel, G., 1965. The mechanism of faulting in clay experiments. Tectonophysics 2, 343–393.

Paris, J.-P., Mouline, M., Delsahut, B., Durand-Delga, M., Olivier, P., Collomb, P., Gras, H., Roche, J., 1989. Carte géologique de la France (1/50,000), feuille Albi (932), Bureau de Recherches Géologiques et Minières, Orléans (France). Notice explicative par Collomb, P., Gras, H., Durand-Delga, M., Delsahut, B., Cubaynes, R., Mouline, P., Paris, J.P., 56 pp.

Pélissié, Th., 1982. Le Causse jurassique de Limogne-en-Quercy: stratigraphie, Sédimentologie, Structure. Thèse 3ème Cycle, Toulouse, 281 pp.

Prandtl, L., 1924. Spannungsverteilung in plastichen körpen. Proceedings of the First International Congress on Applied Mechanics, Delft, pp. 41–54.

Ramsay, J.G., Huber, M.I., 1987. Modern Structural Geology, Vol. 2: Fold and Fractures. Academic Press, London, pp. 309–700.

Richard, P., Cobbold, P., 1989. Structures en fleur positives et décrochements crustaux: modélisation analogique et interprétation mécanique. Comptes Rendus de l'Académie des Sciences de Paris 308 (II), 553–560.

Rolando, J.-P., 1988. Sédimentologie et stratigraphie du bassin permien de Saint-Affrique. Un exemple de bassin alluvial contrôlé par la tectonique extensive. Thèse Université Toulouse, 226 pp.

Rolando, J.-P., Doubinger, J., Bourges, P., Legrand, X., 1989. Identification de l'Autunien supérieur, du Saxonien et du Thuringien inférieur dans le bassin de Saint-Affrique (Aveyron, France). Corrélations séquentielles et chronostratigraphiques avec

les bassins de Lodève (Hérault) et Rodez (Aveyron). Comptes Rendus de l'Académie des Sciences de Paris 307 (II), 1459–1464.
Soula, J.-C., Lamouroux, C., Viallard, P., Bessière, G., Debat, P., Ferret, B., 1986. The mylonite zones in the Pyrenees and their place in the Alpine tectonic evolution. Tectonophysics 129, 115–147.
Tapponnier, P., Molnar, P., 1976. Slip-line field theory and large-scale continental tectonics. Nature 264, 319–324.
Varnes, D.J., 1962. The South Silverton mining area, San Juan County, Colorado; Part D: Analysis of plastic deformation according to von Mises' theory with application to the South Silverton area, San Juan County, Colorado. U.S. Geological Survey Professional Paper, 378 B, 49 pp.
Viallard, P., 1985. Hypothèse sur la polarité des déformations alpines aux marges 'pyrénéennes' des plaques Europe et Ibérie. Comptes Rendus de l'Académie des Sciences de Paris 300 (II), 1019–1024.